CRACK PROPAGATION CHARACTERISTICS IN THE NOZZLE CORNERS OF A PRESSURE VESSEL STEEL MODEL OF LIGHT WATER REACTOR

S. MIYAZONO, K. SHIBATA

Mechanical Strength and Structure Laboratory, Tokai Research Establishment, Japan Atomic Energy Research Institute Tokai-mura, Naka-gun, Ibaraki-ken, Japan

SUMMARY

In light water reactor technology, it is a very important subject that the crack initiation life and propagation behavior is experimentally and theoretically investigated at the nozzles attached to the pressure vessel, where the maximum circumferential stresses are caused at the inner corner surface by internal pressure.

The present paper describes experimental results which were obtained by measuring the propagation length from an artificial crack in the inner corner surface of the nozzles using an electrical resistance method and crack gage, when internal pressure was cyclically loaded to a steel model of reactor pressure vessels. In order to investigate the effects of the shape of nozzles and artificial cracks on the crack initiation life and propagation rate, in this experiment four different shapes of nozzles (each diameter ratio of nozzle to shell is 0.045, 0.075, 0.10 and 0.15) were attached to the pressure vessel model and two different types of artificial cracks (the shape of each crack tip is curved (A-type) and straight (B-type)) perpendicular to the direction of the maximum circumferential stresses were machined at the inner corner surface of each nozzle.

From this experiment, it was apparent that the crack initiation life for the crack tip of A-type was shorter than for that of B-type in every nozzle and for the crack initiation life at each inner surface of nozzle and shell there was not any distinct difference between A and B. The crack propagation rate from the crack tip was initially very large for all artificial cracks with number of cycles after crack initiation to reach a maximum value, it decreased also rapidly until each crack attained the surface tip of each artifical crack and increased with the crack length after that. After each crack passed the surface tip of each artificial crack, it propagated dependent on the diameter and thickness ratio of nozzle to shell, i.e., the crack propagation rate increased generally with increase of their ratios. The tendency was consistent with the magnitude of the circumferential stresses with increasing the diameter ratio of nozzle to shell at the vicinity of the inner corner surface of each nozzle.

To compare these experimental results with the theoretical analysis, it is now being provided to compute the stress intensity factor of each nozzle by a semi-analytical procedure.

1. Introduction

At the inner corners of inlet and outlet nozzles of primary coolant of light water reactor vessels, the highest circumferential stresses are usually caused while internal pressure is given to them in the operation period. Also, their stresses occur cyclically by internal pressure when nuclear reactors are start-up and shut-down or scrummed during their life. Therefore, it is a very important subject to see the crack initiation life and the crack propagation rate at the nozzle corner when cyclic internal pressures are applied to the reactor pressure vessel.

In the authors' laboratory[1),2)] had been carried out low cycle fatigue tests to assess the integrity of Japan Power Demonstration Reactor (JPDR) pressure vessel by half and one-third pressure vessel models, in which artificial cracks (notches) were machined at the inner corner surface of the forced circulation nozzle where the maximum circumferential stresses were caused usually by internal pressure. In these tests the crack propagation length from the notches had been continuously measured by a electric resistance method and crack gages. The crack initiation life and propagation rate at the nozzles of every pressure vessel model were obtained and from the experimental results was estimated the crack propagation behavior at the forced circulation nozzle of JPDR.

Recently in order to see the crack propagation growth at the nozzles of light water reactors, some investigations[3),4),5)] have been carried out by applying fracture mechanics to this subject. Then, the stress intensity factor at the crack tip of nozzle corners has been obtained experimentally and also some computations have been attempted to investigate it theoretically.

2. Experimental procedures

2.1 Pressure Vessel Model

The pressure vessel model used in this experiment is shown in Fig.1 and the mechanical properties of the materials of the shell and nozzle in Table 1. The shell was made by a low carbon steel, ASTM Type A302 Gr.C and the nozzle by a forged steel, ASTM Type A336 Modified. To the vessel model were attached four kinds of nozzles which had the diameter ratio of nozzle to shell of 0.045, 0.075, 0.100 and 0.150 respectively, as shown in Table 2. The diameter ratio was determined based on the ratio of nozzle to shell diameter of the pressure vessels for boiling water reactors which have been practically operated or designed at the present. Some examples of nuclear power plants are denoted in Table 2, but No.4 nozzle of the ratio of 0.150 was attached to the vessel model for comparison with other three nozzles. The detail of each nozzle is shown in Fig. 2-(a),-(b),-(c) and-(d).

2.2 Static Internal Pressure Test

In order to obtain the stress distributions at the inner and outer surface of each nozzle, many strain gages of rosette type were attached to each place, for example, as denoted in Fig. 3-(a) and-(b). The static internal pressure were given gradually by oil to maximum 120 kg/cm^2 which was selected to compare with the experimental results of No.1 pressure vessel model tested before.

2.3 Artificial Cracks

After the static internal pressure test, two kinds of artificial cracks (notches)

perpendicular to the direction of maximum circumferential stresses were machined at the inner corner surface of each nozzle by a thin grinder of 0.3 mm thickness and 30 φmm diameter. One is A type notch, the tip of which was machined bowedly along the inner surface of the corner of each nozzle and another is B type notch, the tip of which was made straight, as shown in Fig. 2. The depth of A type notch was 3 mm and the length of the inner surface was 40 mm, while the depth of B type notch was also 3 mm and the length of the inner surface was different every nozzle. The detail of each notch is also depicted in Fig. 2. These two types of notches were machined symmetrically both flange and bottom side of the model, parallel to the axis of the shell, at the inner corner of each nozzle to investigate the effect of notch shape on the crack initiation life and propagation rate, but in No.1 nozzle only B type notch was prepared because the machining was very difficult due to its small diameter.

2.4 Cyclic Internal Pressure Test

The cyclic internal pressure was applied to the pressure vessel model by the cyclic rate of 5 c.p.m from 1.5 to 120 kg/cm^2 after two artificial cracks were machined at the inner corner of each nozzle. The crack initiation life and crack propagation length from these notches were measured continuously to the direction of the depth (θ = 45°) by an electrical resistance method and at the inner surface of the shell (θ = 0°) and nozzle side (θ = 90°) by crack gages. The internal pressure had been applied cyclically to the leakage of oil from one of four nozzles.

3. Experimental Results

3.1 Stress Distributions at the Inner and Outer Surface of Nozzles

All the stresses of each place were calculated as elastic values from the strains obtained in the static internal pressure test of 120 kg/cm^2 by general expressions between stress and strain. In this case, as Young's modulus and Poisson' ratio were used E=2.1x10^4 kg/mm^2 and ν = 0.3 respectively. As an example, in Fig. 3-(a) and-(b) are shown the stress distributions at the inner and outer surface of No.4 nozzle. The maximum circumferential stresses were caused at the inner corner of each nozzle where almost the same maximum stresses were obtained at the symmerical two points, as denoted in Fig. 3. On the other hand, the maximum stress values of axial direction at the inner surface and ones of circumferential and axial direction at the outer surface were less than ones of circumferential direction at the inner surface. Almost the same experimental results were obtained also about other three nozzles. The stress concentration factors of maximum circumferential stresses at the inner corner of each nozzle were 2.9, 2.8, 2.9 and 3.1 respectively.

3.2 Crack Initiation Life and Crack Propagation Behavior

The crack initiation life in the direction of θ = 45° of A and B type notches was shorter than one at the inner surface of shell (θ = 0°) and nozzle side (θ = 90°) of both notches, as shown in Fig. 4 and 5. Meanwhile, it was clear as shown in Fig. 4 that there was a little difference between A and B type notch about the crack initiation life in the direction of θ = 45° of each notch. Any distinct differences between A and B type notch could not be found about the crack initiation life at the inner surface of θ = 0°, as denoted in Fig. 5. Also at the inner surface of θ = 90° there were not any evident differences

between both notches about the crack initiation life.

On the other hand, it was clear as in Fig. 4 and 5 that A and B type notches showed quite different crack propagation behavior until all the cracks passed through the tip of each notch and after that there was a little difference of the crack growth between A and B type notch. Since the crack initiation life of A type notch was shorter than one of B type notch, however, it was found that the crack propagation length of A type notch was longer than one of B type notch when the cyclic internal pressure test was stopped because of oil leakage. It occurred at the outer surface of No.4 nozzle with A type notch due to the crack perforation after cyclic internal pressure of 20,900 cycles. The photograph of cross section of No.4 nozzle is shown in Fig. 6 and its drawing in Fig. 7, in which the machined notch, fatigue failure surface, artificial fracture surface and machined surface are depicted to explain every part of the photograph. As shown in these two figures, the crack propagation length of A type notch was longer than one of B type notch and the same experimental results were obtained also about other three nozzles. In No.1 nozzle, however, there was only a little difference of crack propagation length between flange and bottom side because they were the same notches of B type.

It was found from these experimental results that the crack propagation behavior was dependent on the diameter ratio and thickness ratio of nozzle to shell, that is, the larger their ratios were, the longer the crack propagation length was both A and B type notches as shown in Fig. 4 and 5.

4. Discussions and Conclusions

In Fig. 8 and 9 are shown the relations between crack propagation rate, $\frac{da}{dN}$, in the direction of $\theta = 45^\circ$ and number of cycles, N, of both A and B type notches. Here a shows the crack propagation length at the direction of $\theta = 45^\circ$. Their crack propagation rates increased suddenly after the crack initiation, but they gradually approached to constant values at any number of cycles and after that decreased with number of cycles. It seems that the crack propagation rates increased very hastily nearly to the tip of each notch, influenced intensely by the large circumferential tensile stress at the inner corner of each nozzle and decreased near the tip of each notch due to the complicated three-dimensinal stress distribution. After the cracks passed through the tip of each notch, they increased gradually with number of cycles. As shown in Fig. 8 and 9, the crack propagation behavior of A type notch was quite different with one of B type notch and the former increased more hastily than the latter until the crack passed through the tip of each notch, although there was the same tendency between them. It was, however, found that A type notch was nearly equal to B type notch after that.

The relations between crack propation rate, $\frac{dls}{dN}$, at the surface of shell side ($\theta = 0^\circ$) and number of cycles, N, of both A an B type notches are depicted in Fig. 10 and 11 which show the crack propagation behavior after the cracks passed through the tip of each notch. Here ls shows the crack propagation length at the direction of shell side ($\theta = 0^\circ$). The crack propagation rates of A type notch were larger than ones of B type notch at the surface of shell side, but there was a little difference of them between both notches. From these experimental results, it was evident that the crack propagation rate of A type notch was

quite different with one of B type notch until the crack passed through the tip of each notch, since it seems that different stress distributions were caused near the inner corner of each nozzle dependent on the notch shape. After that the crack propagation behavior of A type notch was almost of the same with one of B type notch in three directions of θ = 0°, 45° and 90°, although the crack propagation length was different between A and B type notch dependent on their crack initiation life.

The crack propagation rate in three directions of both A and B type notches was dependent on the diameter ratio of shell and nozzle, d/D, and the thickness ratio of shell and nozzle, t/T. Here d, D, t and T show the diameter of nozzle and shell and thickness of nozzle and shell respectively. It was found that the rate increased usually with increase of d/D and t/T, although this relation was not entirely clear between No.2 and No.3 nozzle. Then, it seems that the crack propagation rate was dependent on the circumferential stress distributions near the inner corner of each nozzle, as shown in Fig. 12, which were obtained by static internal pressure before the artificial cracks were given to it. That is, the crack propagation rate increased with increase of the circumferential stresses near the inner corner.

Acknowledgement

The authors wish to acknowledge Dr. T. Fujimura, Technical Research Association for Integrity of Structures at Elevated Service Temperatures (ISES) for his helpful suggestions and discussions for this subject and also thank Mr. T. Oba, Mr. R. Kawamura and Mr. Matsumoto for their collaboration and assistance.

References

(1) Fujimura, T., Miyazono, S., Ueda, S., and etc., "Characteristics of Crack Propagation in Overlaid Nozzles of a Nuclear Reactor", Ist Intl. Conf. on Pressure Vessel Tech., Delft, The Netherlands, September 29-Oct. 2, 1969, 2-94, p.1213-1220.

(2) Fujimura, T., Miyazono, S., Kodaira, T. and Shibata, K., "Integrity Assessment of Structural Models of a Reactor Vessel with Notched Nozzles under Cyclic Pressure Loading", 2nd Intl., Conf. on Pressure Vessel Tech., San Antonio, Texas U.S.A., Oct. 1-4, 1974, 2-58, p.801-819.

(3) Derby, R. W., "Shape Factors for Nozzle Corner Cracks obtained from Epoxy Model Pressure Vessels", HSST 6th Anu. Inf. Meeting, Oak Ridge, Tennessee U.S.A., April 25-26, 1972, No.17.

(4) Ruiz, C., "Stress Intensity factors for nozzle corner cracks", Strain, Janu. 1973, p. 1-3.

(5) Broekhoven, M. J. G., "Analysis of a Nozzle-Corner Crack Problem", 2nd Intl. Conf. on Structural Mechanics in Reactor Technology, Berlin, Germany, September 10-14, 1973,G4/7.

Item	Material	Yield strength (kg/mm^2)	Tensile strength (kg/mm^2)	Elongation (%)
Shell	A302C	52.4	67.5	19.2
Nozzle	A336	37.1	57.0	22.9

Table 1 Mechanical properties of the materials of shell and nozzle of pressure vessel model

Nozzle number	Ratio of nozzle to shell diameter for model (di / Di)	Ratio of nozzle to shell diameter for BWR pressure vessel (di / Di)		
		460 MW	700 MW	1,000 MW
1	0.045	Core spray nozzle $\frac{di}{Di} = \frac{219}{4793} = 0.0457$	Core spray nozzle $\frac{di}{Di} = \frac{272}{5538} = 0.0492$	Water supply nozzle $\frac{di}{Di} = \frac{300}{6376} = 0.047$
2	0.075	Outlet nozzle of steam $\frac{di}{Di} = \frac{363.6}{4793} = 0.0758$		
3	0.100		Outlet nozzle of steam $\frac{di}{Di} = \frac{566.6}{5538} = 0.102$	Outlet nozzle of steam $\frac{di}{Di} = \frac{613.8}{6376} = 0.0962$
4	0.150			

Table 2 Diameter ratio of nozzle to shell of light water reactor pressure vessels and pressure vessel steel model

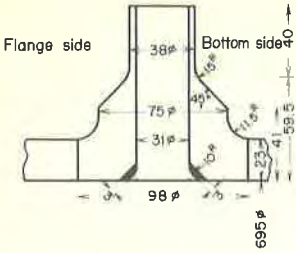

(a) No.1 nozzle

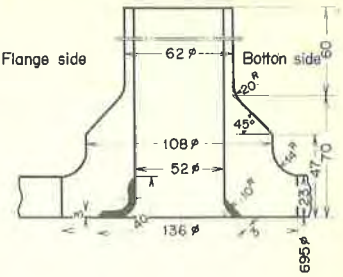

(b) No.2 nozzle

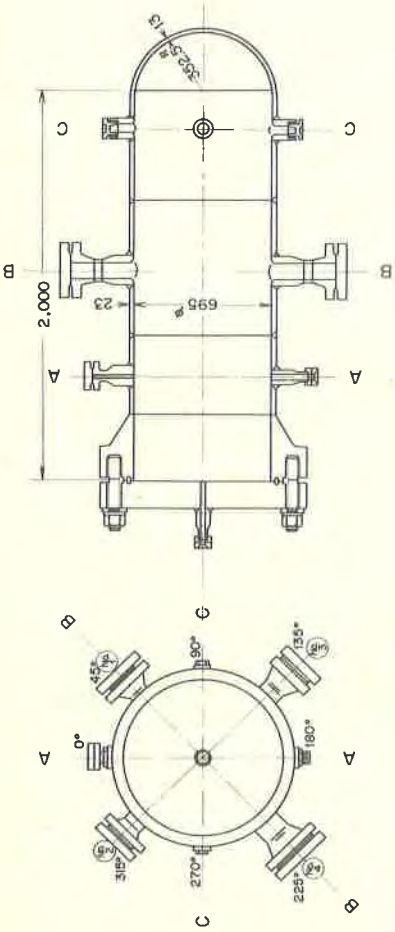

Fig. 1 Pressure vessel steel model of light water reactor

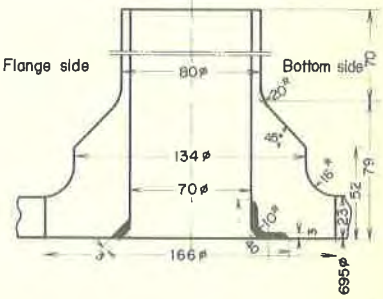

(c) No.3 nozzle

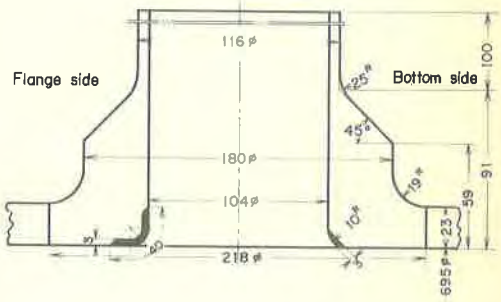

(d) No.4 nozzle

Fig. 2 Detail of No.1, No.2, No.3 and No.4 nozzle and of A and B type notch (artificial crack)

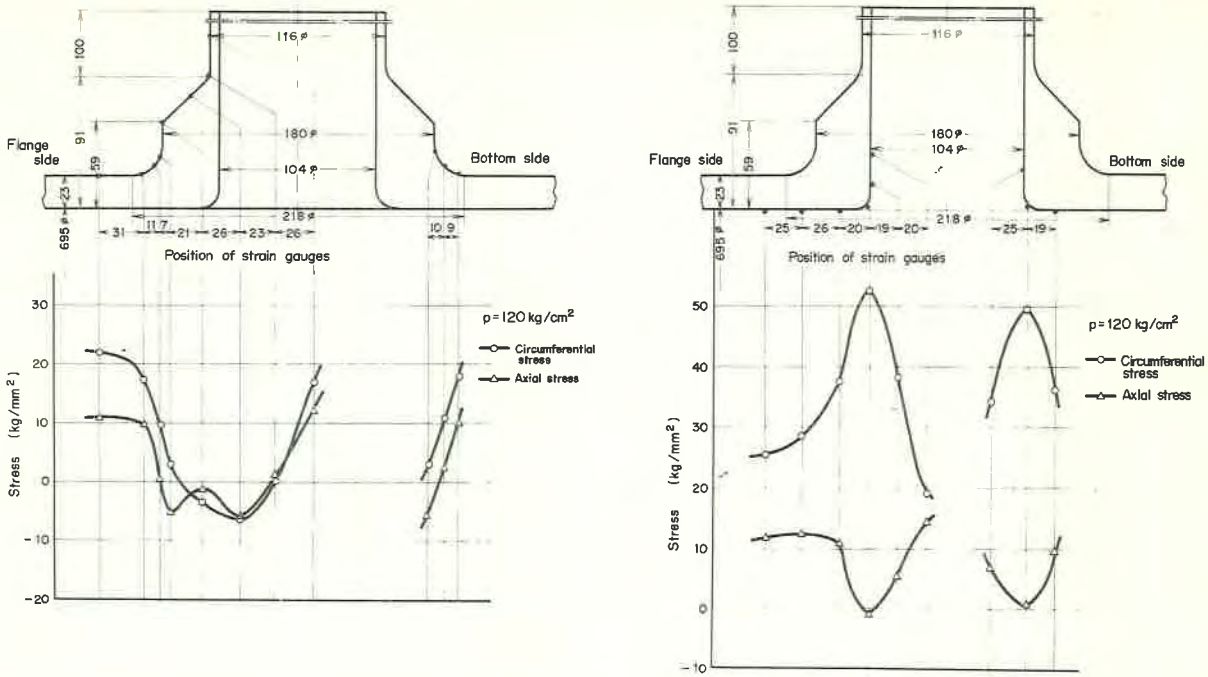

Fig. 3 Stress distribution at the inner and outer surface of No.4 nozzle

(a) Inner surface

(b) Outer surface

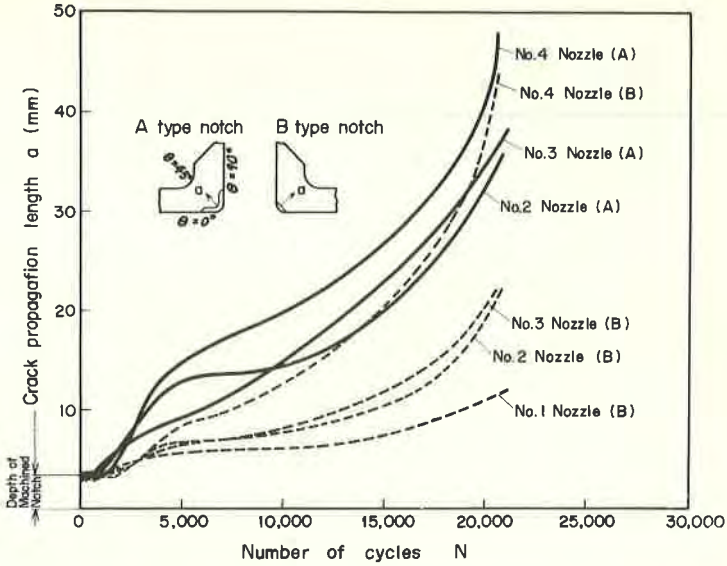

Fig. 4 Relation between crack propagation length and number of cycles at the direction of θ = 45°

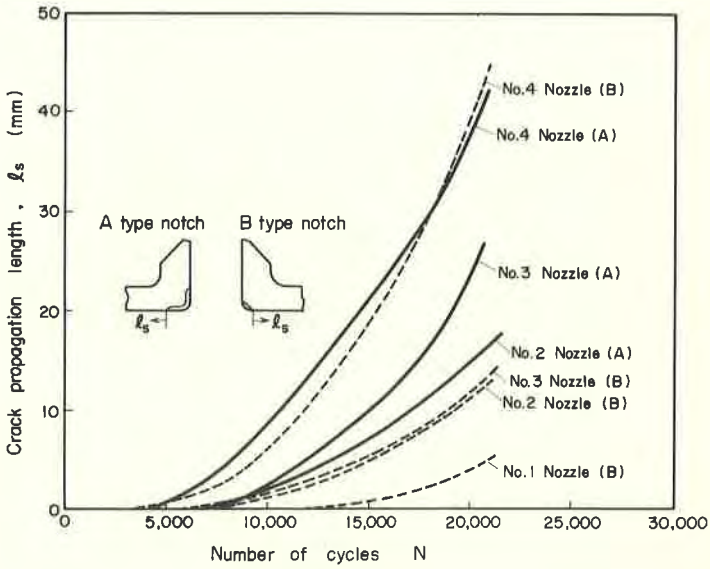

Fig. 5 Relation between crack propagation length and number of cycles at the inner surface of θ = 0°

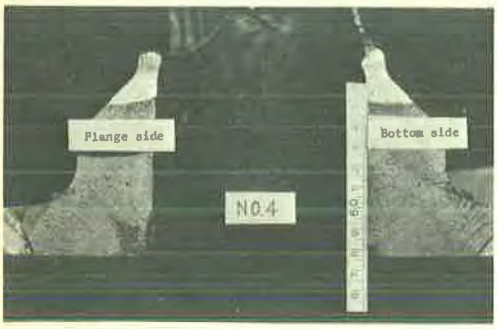

Fig. 6 Photograph of cross section of No.4 nozzle after fatigue failure

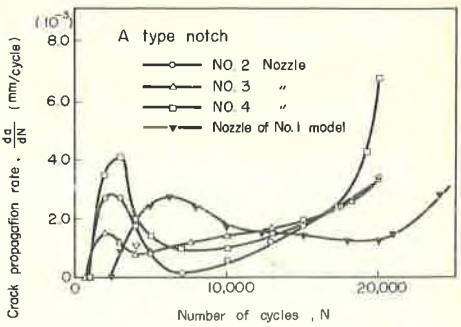

Fig. 8 Relation between crack propagation rate and number of cycles at the direction of $\theta = 45°$ of A type notch

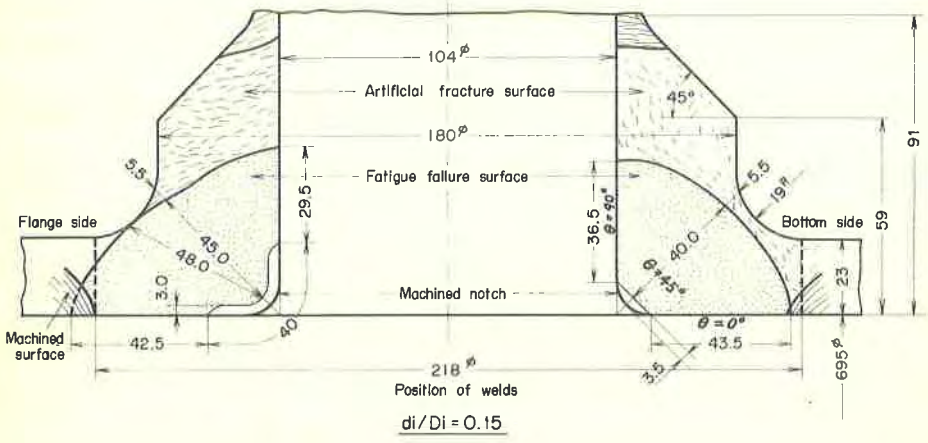

Fig. 7 Drawing of cross section of No.4 nozzle after fatigue failure

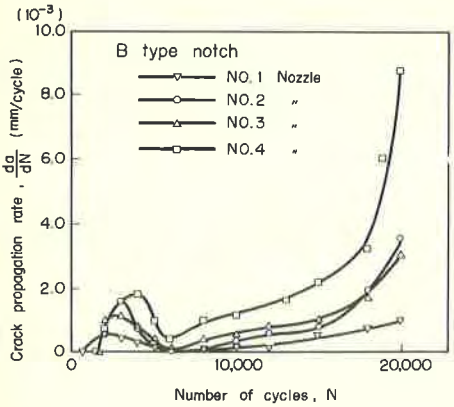

Fig. 9 Relation between crack propagation rate and number of cycles at the direction of $\theta = 45^\circ$ of B type notch

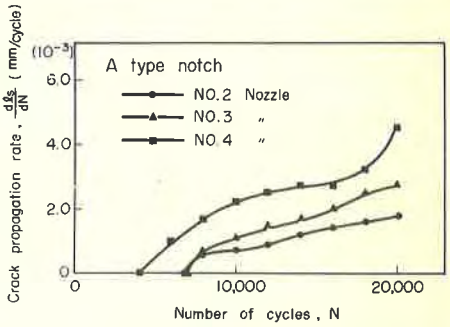

Fig. 10 Relation between crack propagation rate and number of cycles at the inner surface of $\theta = 0^\circ$ of A type notch

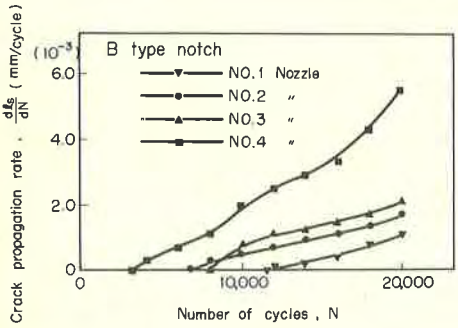

Fig. 11 Relation between crack propagation rate and number of cycles at the inner surface of $\theta = 0^\circ$ of B type notch

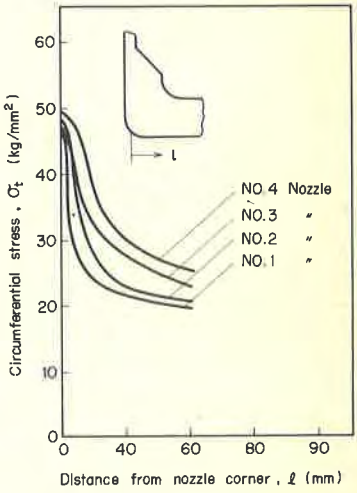

Fig. 12 Circumferential stress distribution at the inner surface corner of each nozzle